Structures and flows in the solar active photosphere and chromosphere

G. Tsiropoula

Institute of Space Research, National Observatory of Athens, Lofos Koufos, 15236 Palea Penteli, Greece

Abstract. Solar activity is the result of the coupling of the magnetic field with convection and differential rotation. The great variety of features observed in the solar atmosphere is due to the presence of this magnetic field, embedded in a highly conducting plasma. The individual structures comprising the photospheric and chromospheric active regions occur at different spatial and temporal scales, are controlled by different physical mechanisms and have different physical properties. There is a general consensus that understanding of their properties and their behaviour is a key in obtaining a view of the Sun as an integral physical system. Among these properties, mass motions are considered to be very important and their diagnosis is crucial, since they are related to fundamental physical processes. Observations from both ground-based and space-borne experiments and interpretation techniques are advancing our knowledge on the properties of the different structural forms, including their flow patterns. Since it is impossible to give a full account of the existing observational and theoretical results, we shall concentrate in this review to present methods used for the determination of the velocities and to give a summary of some important properties of these structures, including their velocity fields.

1. Introduction

During IAU Symposium 35, K. O. Kiepenheuer (1968) defined an active region as "The totality of all observable phenomena preceding, accompanying and following the birth of sunspots, including radio-, X-, EUV and particle emission". This is not surprising, since the study of sunspot structure constituted the first research on solar activity. With the high spatial resolution of the current solar observations achieved both from the ground and from space we have now a more complete picture of the highly structured topography of the different solar layers. Even more, it is now well established that the variety in morphology of the various structural components originates in the difference of the strength and inclination of the magnetic field. Thus it becomes necessary to extend the above definition of an active region. Nowadays, the criterion that distinguishes an "active" from a "quiet" region is the presence or absence of strong magnetic field. It should be noticed that the terms "active" or "quiet" are sometimes used loosely and without consistency from layer to layer. But, in general, active

regions differ from quiet regions or from coronal holes in these respects: (1) they contain more magnetic flux and have more complicated fine structure, (2) a larger fraction of the magnetic field lines is closed and (3) they contain more non-thermal particles, as evidenced by non-thermal radio emissions.

It is well known that the great variety of the dynamic phenomena which make up the solar activity is basically due to the interaction of magnetic field with convection and differential rotation. The role of the convective processes is to bring together the magnetic field lines that emerge from the Sun's interior into concentrated flux tubes. This concentration of magnetic fields leads to several completely different structural forms in the photosphere and chromosphere. In the photosphere, active regions manifest themselves as faculae, pores and sunspots; in the chromosphere as extended bright plages, sunspots (and phenomena occurring in their neighbourhood and often related with them, such as the powerful explosions observed as flares, arch filament systems, fibrils etc) and filaments.

Understanding the solar atmosphere as a whole presupposes the knowledge of the physical properties (lifetimes, mass motions, heating and cooling, etc) of the various individual structures. Among these properties the importance of mass motions seems self-evident as they are a signature of mass and energy transport and dissipation. Motions over all spatial scales are observed, since even the global solar atmosphere per se shows not a static but a dynamic behaviour.

In this review we cannot give a full description and explanation of the features and their properties. Among the topics we do not touch upon are sunspots, which have been the subject of the 1st Advances in Solar Physics Euroconference and eruptive chromospheric phenomena like flares, surges and sprays. We will present methods used for the velocity determination and the flows, both horizontal and vertical, observed in these two layers of the solar atmosphere. We will describe properties of these structures for which it appears that observations have given definitive answers, but we also point out several open questions waiting for improved observations and/or interpretations.

2. The solar photosphere and chromosphere

2.1. Spectroscopic diagnostics

In order to obtain a detailed picture of the solar structured photosphere and chromosphere, observations in lines and continua at different wavelengths are used. The observation of the shapes and intensities of spectral lines and their interpretation poses a major challenge because they provide a lot of information about the dynamic processes in the Sun. Not all lines are formed by the same process. In the photosphere LTE is usually assumed. In this case the source function (and the radiation in the continuum) is equal to the Planck function which is very sensitive to the temperature. In the chromosphere LTE can no longer be assumed and appropriate techniques are required to extract information on the different physical quantities. A broad distinction can be made between lines that are controlled by collisions (such as the Ly-α, Ca II and Mg II lines), which provide information on the physical conditions in the emitting region and lines such as Hα that are photo-ionization controlled. These latter

lines are not very sensitive to the physical conditions in their region of formation but depend strongly on the radiation field.

2.2. Velocity diagnostics

The methods employed for the observation and study of velocity field and the instruments involved are usually not simple. From the study of motions as a function of space and time flow patterns are deduced. For the derivation of these flow patterns four independent variables are important: the spatial coordinates x, y, the wavelength λ and the time, t. According to the kind of observation performed and the kind of data needed, different optical systems with additional equipment and various scanning possibilities have been invented (Wöhl 1992, Mein 1992). The new generation of imaging solar experiments use solid state digital imaging detectors or filter camera systems, video cameras etc.

Instrumentation

Several instruments are used for solar observations. We shall describe briefly some of them.

1. White light imaging camera

This camera provides white light images which are in general taken in a small spectral region around 5000 to 6000 Å in between the Ca II K (3934 Å) and the Hα (6563 Å) lines. These images are usually used for the determination of horizontal velocities. *2. Filtergraphs*

Using filter techniques we have the possibility to obtain temporal sets of filtergrams in Hα or movies (Big Bear Solar Observatory, Meudon 3λ heliograph, Astronomical Observatory of Wroclaw University). Filtergrams provide apparent motions of chromospheric material. Special attention should be paid to the interpretation of such motions especially when these structures are observed at the limb, because they may be the effect not only of Doppler motions but also of variations of the ionization degree of the material with time or of wave propagation through the atmosphere.

3. Spectrographs

Quantitative Doppler shift velocities are best obtained with spectrographs, because generally the wavelength scale is calibrated and the velocities are accurate. Spectrographs can observe in several chromospheric lines such as Hα, Ca II H and K lines, He lines. They are installed, among others, at the following telescopes: the Oslo Solar telescope, the Sac Peak Solar Vacuum telescope, Hida Solar Tower in Kyoto, MacMath telescope at Kitt Peak Observatory. The best spatial resolution along the slit is about $0.5''$, but it is very often reduced because of the seeing conditions.

3. Multichannel Double Pass Spectrograph (MSDP)

The (MSDP) provides sufficient spectral information for relatively broad lines, such as Hα, and has been used efficiently for studies of chromospheric structures. This instrument records a 2D field of view of a solar region at several wavelengths along the line profile. It was first developed at the Meudon Solar Tower, providing 9 spectral channels over the Hα profile and an elementary field of view equal to $1'\times8'$ (Mein 1977). It is also installed on the 50 cm refractor of the Pic du Midi Observatory providing 11 channels and $45''\times5'$ field of view and more recently on the VTT and on the THEMIS telescopes operating on the Canary Islands (with 9 and 22 channels respectively, 2 lines simultaneously and

using a CCD camera (Mein 1991)). The profile of the Hα line is reconstructed taking into account photometric corrections and calibrations. By displacing the entrance slit a large region can be covered quickly in several wavelengths and this is one of the main advantages of the MSDP spectrograph.

5. Doppler compensator

This instrument allows to investigate the amount and sign of the shifts of spectral lines, when the complete profiles of the lines are not needed. The Doppler compensator was invented to keep a magnetically sensitive spectral line centered on the slits, so that the polarization could be measured. Later it was used for determinations of the velocity fields. The most known instrument of this type is the one of the Mt Wilson which performs magnetic field and Doppler velocity measurements. The smaller shifts measured are of the order of about 10 m s^{-1}.

Techniques for velocity determination

1. Horizontal flows

Two main techniques are available to follow the horizontal surface motions: the local correlation tracking, and a simulation procedure of the motion of test particles ("corks").

(i) *Local correlation tracking* is used for the measurement of velocities perpendicular to the line of sight (November et al 1987, November and Simon 1988, Spruit et al 1990). This technique is usually used for tracking photospheric structures, but recently there is an attempt to track on chromospheric structures too (Yi and Molowny-Horas 1995). To apply this technique one chooses a reference frame, e.g. the first frame of a time series. A window function (usually a truncated Gaussian) is applied in turn to each mesh point of a regular grid in the reference and subsequent frames and the relative displacement that maximizes the correlation between the small-scale patterns visible in the window is found. The position of the cross-correlation maximum of the small scale patterns in the different frames relative to those in the reference frame yields a local displacement which is a measure of the horizontal flow.

(ii) Another method is to *simulate the transport of matter by the flow*. This is done by adding markers (test particles) uniformly distributed on the first frame of a time series and updating their positions from frame to frame according to the horizontal flow speed calculated by LCT techniques (November et al 1987). These test particles are called *"corks"*. By overlaying the vector flow field and the cork patterns on the original images and viewing the time sequence, it is possible to obtain a qualitative impression of the time evolution of different photospheric structures like facular points, granules, supergranules, etc.

2. Line-of-sight flows

Several diagnostic techniques have been attempted that have proved useful for the detection of the line-of-sight velocity fields on the solar disk. They are based on the Doppler effect of the solar absorption and emission lines. Some of them use inversion techniques of the line profiles to infer the velocity and other physical parameters. A lot of work is based on the analysis of the Hα profile. Recently some approaches have been used to take into account the coupling between dynamics and the multi-dimensional radiative transfer in non-LTE.

(i) Doppler techniques

Doppler shift techniques involve the measurement of the wavelength shift between the centers of a $\Delta\lambda$-wide chord in the observed and a reference profile. This method can give reliable results in the photosphere, but its application is not fully justified in the chromosphere and higher levels, where non-LTE effects and inhomogeneities must be taken into account in the interpretation of line profiles. Caution in the interpretation of observations must also be taken because of errors introduced from spatial, line-of-sight and temporal averaging of Doppler shifts (Beckers 1981). Moreover, solar lines are asymmetric; it is proposed that these asymmetries are mainly caused by a depth gradient of the velocity in the region under study (Kulander & Jefferies 1966).

A simple and frequently used method for inferring the depth variation of the macroscopic velocity field is the so called *bisector method*. The line bisector is the locus of points midway between equal intensity points on either side of the line. A technique based on the *subtraction of photographs* is extensively used for the detection of solar oscillations, but also for the study of dynamic events (Leighton et al 1962, Bray 1973). An image of the Sun taken in the blue side of a line is subtracted from an image taken in the red side of the line. In the resulting image, called a "dopplergram", an outward motion in a region results in an increase in brightness, while an inward motion in a darkening. Dopplergrams give much more information than a single line-wing image. Furthermore, time series of such images allow us to follow the material motion. The ratio usually defined as,

$$A = \frac{I_b - I_r}{I_b + I_r} \tag{1}$$

and called "Doppler signal", is a measure of the doppler shift (the normalization with the sum of the intensities eliminates effects of intensity variations). In a technique based on *the Stokes V profile*, the difference signal between right and left circularly polarized light is used to determine properties of unresolved magnetic areas and for the derivation of doppler shifts (Solanki 1986). The wavelength shift, $\Delta\lambda$, between a zero-crossing wavelength, λ_o, when the plasma is at rest and λ_v, when a line-of-sight velocity is present is related to the velocity of the magnetized plasma (e.g. $v = c\Delta\lambda/\lambda_o$)

(ii) Inversion techniques

In this method the line profile is inverted by adjusting its parameters by an iterative procedure, in order to obtain the best fit between the calculated and the observed profile. Two cases can be distinguished: the *linear case* and the *non-linear case*. In the *linear case* the line profile disturbances can be written as first order expansions of fluctuations of the different quantities (such as pressure, temperature, velocity etc) (Mein 1971). The intensity perturbation $\delta I_\lambda(t)$ which results from small disturbances of any physical quantity can be described by:

$$\delta I_\lambda(t) = \int_{-\infty}^{\infty} W(z)\delta q(z,t)\, dz \tag{2}$$

where $\delta q(z,t)$ is the fluctuation of any physical quantity at a point z in the atmosphere at time t and $W(z)$ is the corresponding Weighting Function. The velocity Weighting Function is also called the Response Function (Beckers & Milkey 1975, Canfield 1976). Weighting Functions have been exhaustively investigated for wave propagation and especially for energy transport in the chromosphere

because their Fourier transform can directly lead to amplitude and phase of the waves (Schmieder et al 1980, Mein et al 1981). The fundamental difficulty of this method is that no theory gives the number of parameters describing the atmosphere which can be determined from a given line profile.

If the amplitude of the disturbance is large enough, *non-linear* effects arise. A *non-linear method* has been applied by Mein et al (1987) to a time sequence of high resolution spectra of the Ca II 3968 Å line. They proposed an inversion method using a "double profile" for fast convergence and second order expansion of Fourier components as functions of disturbances. The temperature and velocity are represented by 2 coefficients (T_1, T_2 and v_1, v_2). These coefficients which give temperature, temperature gradient, velocity and velocity gradient are theoretically associated to the coefficients of the Fourier expansion of the intensity $I(\lambda)$ by second order expansions and are obtained after a few iterations.

(iii) Hα profile analysis

Hα is in general a very broad absorption line. The core is saturated and the line has wings several Å wide. The wings are formed in the upper photosphere, while the core in the chromosphere. Thus, if one has the possibility to observe the entire line profile, one can explore a substantial range of heights in the solar atmosphere. Furthermore Hα observations constitute a significant fraction of solar observations. In order to benefit from the large amount of information contained in them, different methods have been proposed. Most of these methods use an iterative procedure to derive physical parameters useful for the modelling of the different structures.

Since 1964, when Beckers proposed a technique for extracting some quantities from Hα contrast profiles, a method known as *Beckers' cloud model* or *classical cloud model* has been extensively used in the analysis of chromospheric features seen in the Balmer lines (Alissandrakis et al 1990, Tsiropoula et al 1993 and references therein). The cloud model considers the feature as an isolated "cloud", located above a uniform atmosphere. The contrast profile, $C(\Delta\lambda)$, is expressed in terms of four parameters: the source function, S, the line center optical depth, τ_o, the Doppler width, $\Delta\lambda_D$ and the Doppler shift, $\Delta\lambda_I$:

$$C(\Delta\lambda) = \frac{I(\Delta\lambda) - I_o(\Delta\lambda)}{I_o(\Delta\lambda)} = \left(\frac{S}{I_o(\Delta\lambda)} - 1\right)\left(1 - e^{-\tau(\Delta\lambda)}\right) \qquad (3)$$

where $I_o(\Delta\lambda)$ is the reference profile emitted by the background. In addition, one assumes that the wavelength dependence of the optical thickness is gaussian:

$$\tau(\Delta\lambda) = \tau_o e^{-(\frac{\Delta\lambda - \Delta\lambda_I}{\Delta\lambda_D})^2} \qquad (4)$$

and that all four parameters are constant throughout the cloud; a further assumption is that the source function is frequency independent. Under these assumptions and other circumstances stated in Alissandrakis et al (1990), this model can give reliable results non only for these 4 parameters, but also for many other physical quantities (Tsiropoula & Schmieder 1997). The velocity values derived with the cloud model are 2 - 3 times greater than those derived with the Doppler shift method (Figure 1a).

For the application of the cloud model an important step is the choice of the background intensity; velocity values derived with a background profile corresponding to the quiet Sun can be 2 times greater than those derived with an

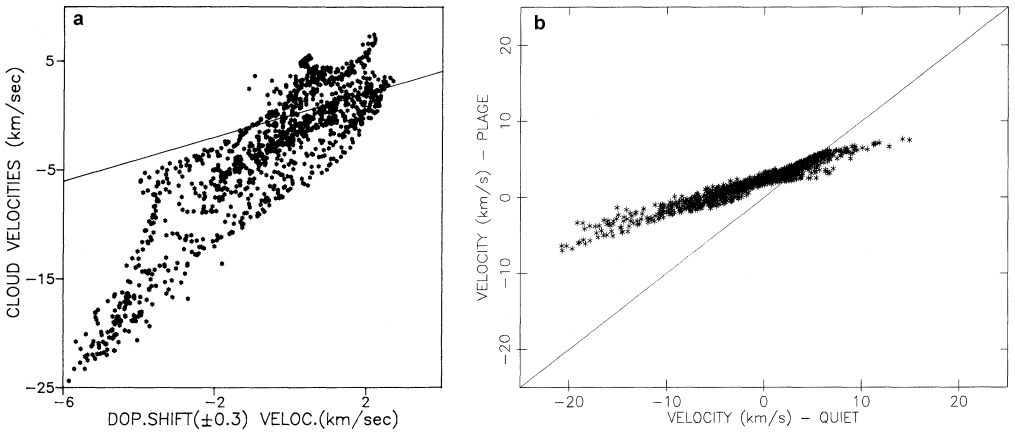

Figure 1. **a** Comparison of the velocities given by the cloud model and the Doppler shift method at Hα $\pm$ 0.3 Å. **b** Comparison of the velocities for two different Hα background profiles corresponding to the quiet and the active Sun (from Alissandrakis et al 1990).

active Sun profile (Figure 1b). The *first order differential cloud model, DCM1,* proposed by Mein & Mein (1988) takes into account the inhomogeneous chromospheric background and can be applied in the case of post-flare loops, in mottles between facular regions etc. If the parameters cannot be assumed constant inside the structure, a method called *second order differential cloud model, DCM2,* has been proposed by the same authors, which takes into account the gradient of the parameters inside the cloud. In the cases where the emission comes from two or more different objects that overlap one another along the line-of-sight like in flares observed on the disk, where ribbons and loops cannot be distinguished from one another, or two mottles overlapping one another, a *"two cloud" model* has been proposed (Heinzel & Schmieder 1994, Gu et al 1997). The emergent radiation after crossing the two clouds is given by:

$$I(\lambda) = I_o(\lambda)\left[e^{-(\tau_1+\tau_2)} - 1\right] + S_1(1 - e^{-\tau_1})e^{-\tau_2} + S_2(1 - e^{-\tau_2}) \qquad (5)$$

where S_1, S_2, τ_1 and τ_2 are the source functions and the optical depths inside the two clouds.

(iv) non-LTE models

A significant step forward in spectral diagnostics of isolated structures is to take into account the coupling between the dynamics and the multi-dimensional radiative transfer in non-LTE. However, it is difficult to apply the non-LTE theory to realistic situations with the necessary rigour, although in recent years various numerical approaches to solve the non-LTE equations have been developed to a high degree of sophistication (Gouttebroze et al 1993, Heinzel 1995, Paletou 1995, Mein et al 1996, Paletou 1996). According to these approaches, given the input parameters T, p, M and ξ_t (T: kinetic temperature, p: gas pressure, M: total column mass ξ_t: microturbulent velocity) the problem of constructing non-LTE models reduces to a solution of the radiative transfer equation for each explicitly treated transition, the set of stationary statistical equilib-

rium equations and constraint equations like total particle number and charge conservation. An important problem difficult to treat is that of the geometry. Gouttebroze et al (1993) computed a set of 140 models of prominences assuming a 1-D vertical slab irradiated symmetrically on both sides. This procedure was also applied to mottles by Heinzel and Schmieder (1994). Horizontal 1-D slabs are also considered which are irradiated only from the bottom (Heinzel 1995, Paletou & Auer 1995, Mein et al 1996). Only recently Paletou (1996) developed a 2-D non-LTE model of prominences which is very promising.

It is thus clear that the derivation of fully consistent results that will correctly describe the variation of the intensity in terms of the velocity and the other physical parameters involved is very complicated and relies in the progress of the theoretical and computational work which will take into account the coupling between dynamics and multi-dimensional radiative transfer in non-LTE.

3. Structures and flows in the active photosphere

In the photospheric layer gas pressure dominates and the magnetic field plays no major role in the structuring of the large scale patterns. However, spatially limited strong magnetic fields in the form of magnetic flux tubes or magnetic elements thread throughout the solar photosphere. Accumulation of magnetic elements produces the photospheric active regions, which manifest themselves as pores, spots and faculae.

3.1. Magnetic elements

It is generally accepted that the active region structures of the solar atmosphere like plages, faculae, filigree and even spots consist of discrete units of strong magnetic field, the *magnetic flux tubes*, which are embedded in a convecting medium with no or very weak field (Stenflo 1973). Outside of sunspots, intense flux tubes carry more than 90 % of the magnetic flux in the photospheric layers of the Sun (Howard & Stenflo 1972). These strong field units are observed as a hierarchy of structures which extend from large active regions with a size of 10^5 km down to smallest magnetic field concentrations with a diameter of a few hundred kilometers and have field strengths in the range of 1 - 3 kG and magnetic fluxes from $\approx 10^{16}$ Mx to $\approx 10^{22}$ Mx.

For the smallest discrete units the term *magnetic elements* is used. The reader is referred to Schüssler (1992) and Solanki (1993) for reviews on this subject. The magnetic elements are considered to be the building blocks of the different magnetic configurations observed in the solar atmosphere. Their role is crucial not only in local active region emergence and decay (Muller & Mena 1987), but also in the overall evolution and global-scale diffusion of magnetic flux on the Sun associated with the solar magnetic cycle (Wang et al 1989; Sheeley 1992). Furthermore, it is suggested that motions of these small-scale magnetic structures in the photosphere due to topological rearrangement of flux tubes act as guides for MHD waves carrying mechanical energy to heat the chromosphere and corona (Parker 1990; Muller et al 1994).

It is clear that magnetic elements are not static structures. However, their internal motions are not well known due to observational limitations (Figure 2). The initial observations of magnetic elements suggested that they were the site

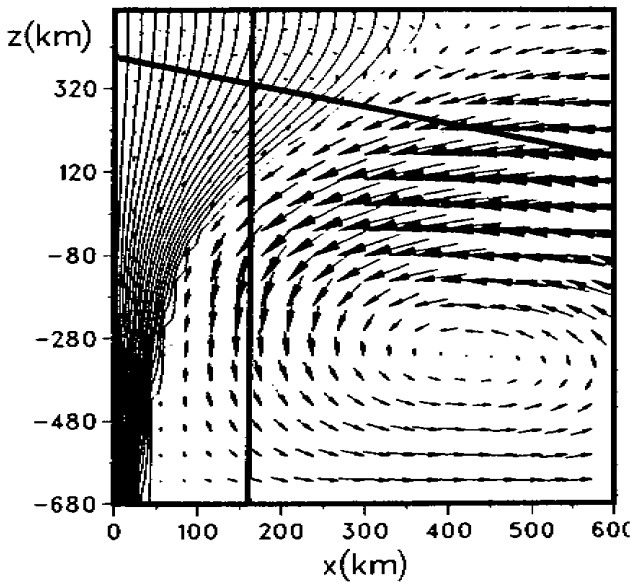

Figure 2. Model of the velocity field of a magnetic element. The two lines-of-sight –one vertical and the other inclined– traverse static, magnetic regions and non-magnetic moving gas leading to Stokes V-profile asymmetries which have different signs (from Schüssler, 1992).

where material is flowing down into the Sun at speeds of about 1 km s^{-1} at photospheric levels. However, this flow needed continuous supply of material into the flux tubes, and this cannot be easily explained by theory. Later observations related the downflows not with the magnetic structure itself but with the surrounding unmagnetized plasma (Frazier & Stenflo 1978, Koutchmy & Stellmacher 1978, Stenflo & Harvey 1985), while Stenflo et al (1984), postulated the existence of a gradient in the vertical velocity of material within the flux tube such that the flow almost vanishes at the photospheric level.

Photospheric magnetic structures are referred to by different names, on the basis of their appearance and magnetic flux: bright and more or less circular points, with flux less than 10^{18} Mx are referred to as "facular bright points"; these points make up the small, bright and elongated features found both in quiet and active regions termed "filigree" and the bright patches observed usually near the limb and called "faculae"; small dark magnetic structures with flux of 10^{18} - 10^{19} Mx are called "magnetic knots". Fluxes greater than about 10^{19} Mx lead to dark pores and even greater to spots. Despite their greatly varying appearance, these photospheric structures can all be described by the magnetic flux tube model.

3.2. Facular bright points

Facular bright points have for a long time been suspected to represent the footpoints of magnetic elements in the photosphere. They are associated with kG magnetic fields, and vary in angular size from $0''.2$ to $0''.8$ (Dunn & Zirker 1973, Mehltretter 1974, Muller 1983, Keil & Muller 1983, Berger et al 1985). Muller

(1983) and Keil & Muller (1983) have studied a large number of facular bright points from several high resolution photographs taken at the Pic du Midi Observatory. They deduced a characteristic size of $0''.22$ ($\sim$ 160 km) although bright features as large as $1''$ are not unusual. They estimated the characteristic peak intensity between 1.4 - 1.6 times that of the mean photospheric intensity. Von der Luhe (1994) arrived at the same results using a speckle imaging technique.

An interesting question which often arises, is the relation of these elemental bright structures with the smallest magnetic elements; different imaging efforts and data reduction techniques have been applied by various authors to find a correspondence between them (del Toro Iniesta et al 1990, Yi & Engvold 1993, Berger et al 1995).

Measurements of the contrast of bright points depend critically on spatial resolution. In low resolution observations these features exhibit low or even negative contrast in continuum wavelengths of the visible and infrared (Foukal & Fowler 1984; Topka, Tarbell & Title 1992) near disk center. Their contrast is found to increase from the center of the disk outward reaching a maximum at about $\mu = 0.3$, where it can be 10 % greater than the adjacent quiet photosphere. Closer to the limb the results are somewhat uncertain since, depending on the observations, either an increasing or a decreasing contrast can be found. On the other hand high resolution observations have given contrast values in the range 1.1 to 2 in units of the average continuum intensity of the quiet photosphere.

The center-to-limb variation of the contrast of facular points has been discussed in some detail by Schüssler (1987) and seems to depend on the inclination of the line-of-sight. For small inclinations the hot bottom of the magnetic tube is obscured leading to disappearance of bright points (Muller et al 1989). At large inclinations the bright wall of the flux concentration becomes visible leading to a positive contrast depending on the ratio between size and depth of the concentration (equivalent to the Wilson effect) (Spruit 1976). Finally, the overlapping of the hot upper regions of the bright points near the limb leads to the sharp increase of the contrast (Steiner & Stenflo 1990).

Despite the observational difficulties of the center-to-limb variation of the facular bright points, their first order association with magnetic elements is well established in a qualitative sense with the following remarks: magnetic flux elements exist before and persist after bright points (Title et al 1992, Yi & Engvold 1993) and less than 50 % of the small scale magnetic flux elements are demarcated by bright points (Berger et al 1995).

3.3. Faculae

Photospheric faculae consist of clusters of bright features the bright facular points or facular granules in faculae, as described above (Mehltretter 1974; Muller 1977). The center-to-limb variation of their contrast has the same behaviour as that of individual bright points (Figure 3). About 90 % of the facular area is found to be associated with spots. Such an area appears as a brightening in a sunspot's surroundings, sometimes preceding the spot's appearance and outlasting it by 2-3 times of its lifetime. Then they progressively fragment and disperse due to the supergranular motions.

Observations show that faculae are increasingly brighter than the photosphere when observed in lines formed at increasing heights above $\tau = 1$. The

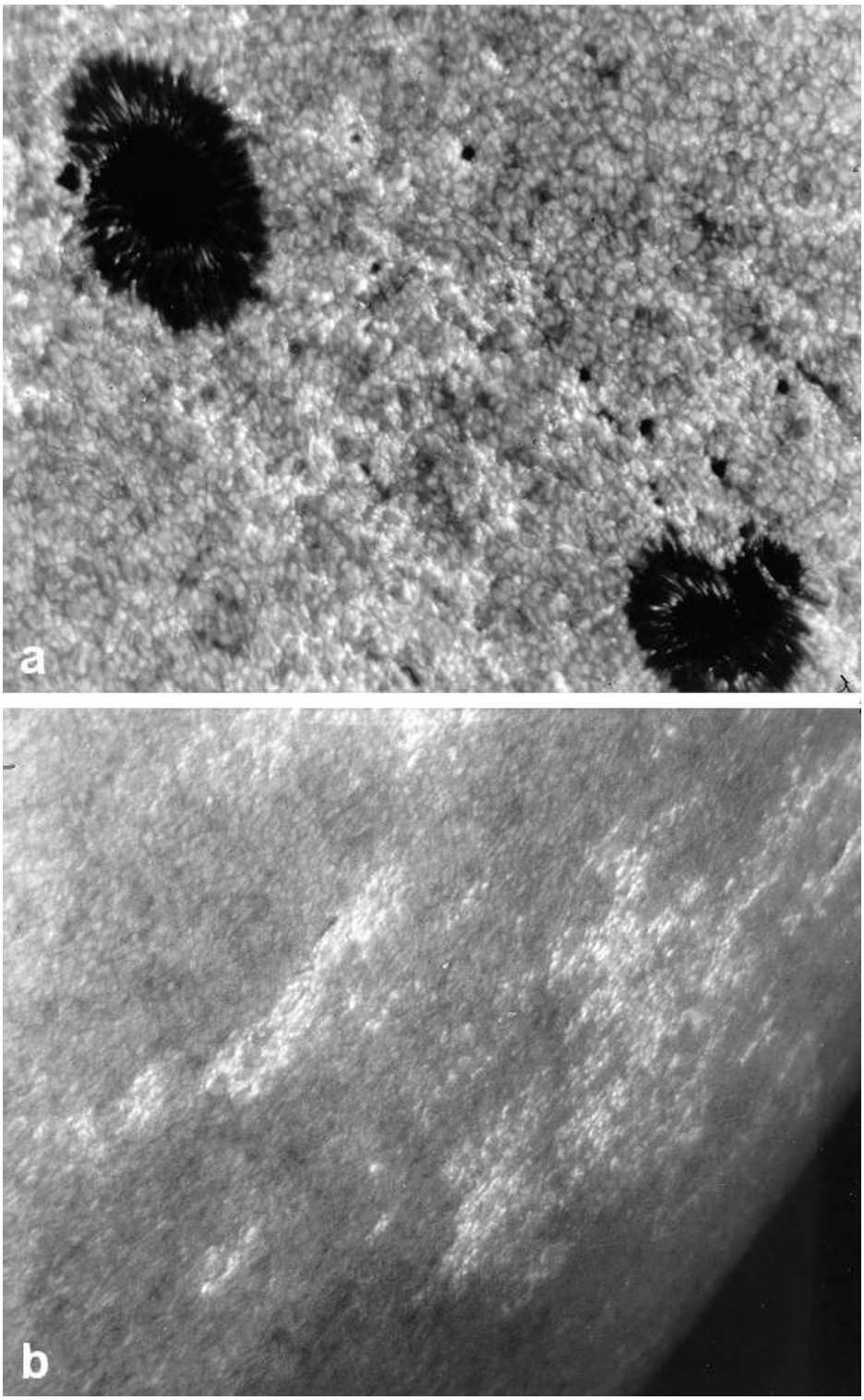

Figure 3. Images of two facular regions obtained at the Pic du Midi Observatory **a** near the disk centre with a G-band filter centered at 4308 Å and **b** near the limb in white light at 5250 Å (Courtesy of R. Muller).

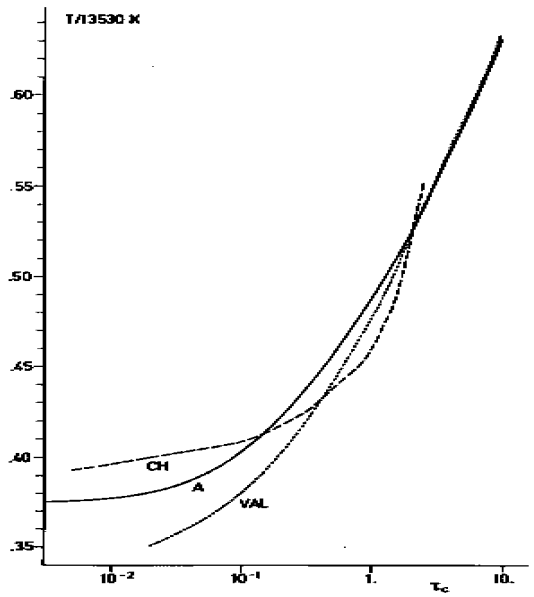

Figure 4. Semi-empirical (CH) and theoretical (A) models of the temperature against continuum optical depth. The photospheric reference atmosphere (VAL) is also plotted (from Deinzer et al 1984).

thermal properties of faculae have been investigated in numerical simulations by various authors (Spruit 1976, Deinzer et al 1984). A semi-empirical model of the temperature distribution based on observations of the Ca K line is shown in Figure 4. The opacity variation from the core to the wings corresponds to a height variation from the chromosphere down to $\tau = 1$. The model shows that at equal optical depths faculae are hotter than the photosphere, while photospheric and facular temperatures converge at about $\tau = 1$. This suggests that the temperature gradient in the facular atmosphere is lower than in the photosphere. However, if the two atmospheres are placed at the same geometrical depth this picture is no more the same. This can be done by shifting the facular atmosphere by a depth equal to the Wilson depression (e.g. $\sim$ 200 - 300 km). Then at all levels faculae are cooler and less dense than their surroundings. The surrounding non-magnetic atmosphere is hotter because convection is not suppressed in it, while the suppression of convective energy transport results in the cooling of the deeper layers.

Faculae are areas of enhanced emission. Besides sunspots, they represent a second component which contributes significantly to the solar irradiance variations, but with the opposite sign. Two important questions have been the subject of several investigations: the first concerns the ratio between a quantity representing the irradiance deficit produced by sunspots and a quantity representing the facular irradiance excess; the second concerns the time scale in which the energy blocked by sunspots is re-emitted by the photospheric faculae. Some authors claim that faculae play a negligible role in the energy balance (Bruning & Labonte 1983, Foukal et al 1983), while others that their role is very impor-

tant (Oster et al 1982, Sofia et al 1982, Steinegger et al 1996a, b). As far as the time scale for the re-emission by faculae of the energy blocked in sunspots is concerned, several contradictory results have been reported. There are authors who claim that faculae re-emit the blocked energy fairly quickly (Oster et al 1982), while others claim that the time scale is comparable to active region lifetimes (Chapman et al 1986) or, even more, equal to months or years (Foukal et al 1983). These discrepancies are due to the different factors entering into the measurements of the two mainly contributing sources to the irradiance variation. In order to get a clear picture of this variation, careful measurements are needed of the area covered by spots and faculae, their temporal evolution, their contrast etc (Steinneger et al 1996b)

Harvey & Martin (1973) found that faculae of opposite polarity move apart with speeds exceeding 2 km s^{-1} during the first half hour, dropping to between 0.7 and 1.3 km s^{-1} during the next six hours or 0.5 km s^{-1} during the first ten hours. Strous et al (1996) found that facular elements constituting a facular region tend to move toward the edge or major sunspot that has the same polarity as their own. Within any small subarea of the active region, facular elements of preceding polarity move toward the major concentrations of preceding polarity and facular elements of following polarity move toward following polarity with a separation velocity of 0.84 ± 0.07 km s^{-1}. Preceding polarity moves faster than following polarity and motions of both polarities are mainly along the E-W direction. Facular elements move faster toward the edges of the active region than those edges move away.

4. Structures and flows in the active chromosphere

The complexity of the solar chromosphere is revealed by high resolution observations in lines formed at different heights above the photosphere. The great variety of the structural forms observed indicate that the physical mechanisms operating in this layer are very different from those in the photosphere. In the chromosphere the magnetic field dominates the gas motions; this is because the photospheric magnetic forces decrease with height with a scale approximately equal to their lateral scale, i.e. thousands of kilometers, while the gas pressure decreases with the barometric scale height, i.e. $\sim$ 100 km.

4.1. Ellerman bombs

Ellerman bombs (EB, also known as moustaches) are narrow structures having an elongated spike-like shape when seen near the limb (Figure 5; Kurokawa et al 1982). They are features of the upper photosphere and lower chromosphere and appear bright when observed in the wings of strong absorption lines such as the Balmer lines, the Ca II H and K lines, and the Na I D and Mg I b lines. Kitai & Muller (1984) showed from a statistical analysis of filtergrams that facular bright points, calcium bright points and EB are different manifestations of the same phenomenon appearing in different layers of the solar atmosphere. Their spectrum shows a strong absorption at the centre of chromospheric lines with extended bright emission in the wings. The maximum of the emission occurs from 0.75 to 2. Å on either side of the line centre and then decreases, until about 7 - 10 Å from the line centre (Severny 1965, Engvold & Maltby 1968).

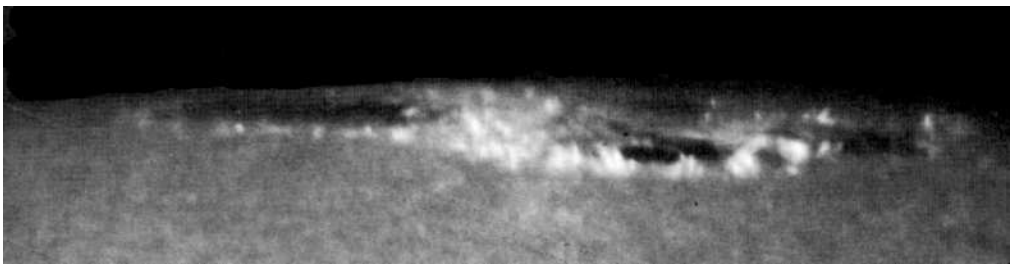

Figure 5. Filtergram at Hα - 1.6 Å of McMath region 16224 on 14 August 1979. Many elongated Ellerman bombs are visible near the solar limb (from Kurokawa et al 1982).

An asymmetry in the wing emission is usually observed with excess emission in the blue (Koval & Severny 1970, Kitai 1983).

Ellerman bombs occur predominantly at the outer borders of the penumbrae of large regular sunspots (under superpenumbral fibrils) and in the interspot region of mature large spotgroups (under Arch Filament Systems) (Bruzek 1968, 1972). An important question is whether Ellerman bombs are flare-like phenomena or they represent an in-situ driven release of energy. Zachariadis et al (1987) found both impulsive and gradual components, with durations of $\sim$ 8 min for the impulsive phase and of $\sim$ 20 min for the gradual phase. As the time curves showed multiple peaks, they suggested that impulsive energy release may occur several times during the lifetime of a bomb. Recently Payne (1993), found time profiles with rapid emission and rapid decay, that are not similar to those of flares. Furthermore, using simultaneous optical, microwave and soft x-ray observations, detected no upper chromospheric or coronal emission associated with Ellerman bombs and concluded that it is not possible to assume a triggering mechanism high in the atmosphere.

The relationship of the EB with the magnetic field has been studied by several investigators with contradictory results due to the lack of high resolution magnetograms. Rust (1968) and Rust & Keil (1992) inferred that EB occur at the polarity reversals of the longitudinal component of the magnetic field, i.e. at the magnetic field reconnection neutral points. Roy & Leparskas (1973) reported that most of the EBs they studied were found at the boundaries of magnetic field concentrations and to the same result arrived Dara et al (1997). Kitai (1983) and Kitai & Muller (1984) considered that EB are isolated flux tubes since they found them in active parts as well as in quiet parts of active regions, where no reconnection of opposite magnetic field lines can occur.

As far as velocities in EB are concerned, Severny (1968) reported upward velocities of 1 - 3 km s^{-1} at photospheric levels. At chromospheric levels Kurokawa et al (1982) found upward velocities of 8 km s^{-1} during the brightening phase of a bomb while Kitai (1983), from an analysis of Doppler shifts of Hα profiles, reported mass motions directed generally upwards with velocities of $\sim$ 6 km s^{-1}. Denker et al (1995) found a correlation between the motions of EBs and granular cells. In particular, they claim that EBs move along the intergranular lanes and are pushed away by large expanding granules with velocities of 1 - 2 km s^{-1}.

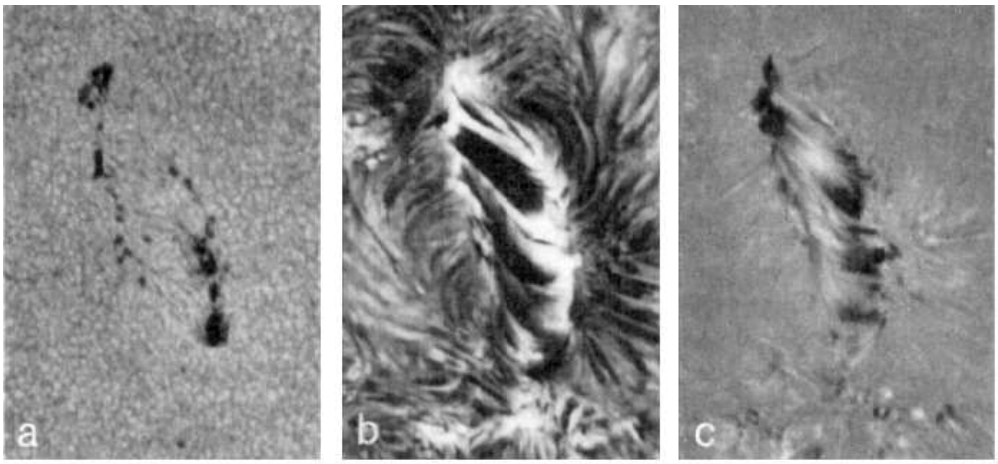

Figure 6. Arch Filament System. **a** In the continuum. Notice the dark alignments in the fuzzy granulation. **b** In the core of Hα. **c** Doppler shift in Hα. The tops of the arches are rising (white), while strong downflows are observed at their footpoints (black). (The images are prepared by L. Strous from data collected at the Swedish Solar Observatory at Roque de Los Muchachos, La Palma by the Lockheed group).

4.2. Arch Filament Systems

The first evolutionary stage of an active region has a characteristic pattern (Emerging Flux Region EFR; Zirin 1972), which takes place on a variety of lengths and time scales and can readily be pictured by the emergence of the top of an Ω-shaped flux loops whose ends are anchored near the bottom of the convection zone (Zwaan 1992). The chromospheric manifestation of an EFR seen in Hα is an arcade of predominantly dark, arch-shaped structures, which spans the neutral line of the magnetic field and apparently traces the lines of force of the emerging magnetic field. These loop-like structures were called *Arch Filament Systems* (AFS) by Bruzek (1967). The AFS are visible for a few days; however the lifetime of an individual AF is estimated to be about 20 to 30 min. Individual arches are fairly narrow ($\sim$ 1000 - 3000 km), while the entire system can reach 15000 - 25000 km. Their mean length is about 30000 km and they can reach a height of 15000 km.

Lower in the atmosphere the emergence of the flux is clearly evidenced from changes in the photospheric granulation (Zwaan 1992, Strous et al 1996). In the central part of the EFR the granulation is disturbed: it looks fuzzy and there are remarkable alignments in the dark intergranular lanes (cf Figure 6a). These dark alignments are parallel to the individual arch filaments and delineate the tops of magnetic loops passing through the photosphere. The magnetic lines of force expand after they emerge out of the photosphere. The rising magnetic arch traps the chromospheric material which also rises, while material is draining down from both feet (Figure 6c). This material, lifted up with the flux rope, scatters the background radiation producing these dark structures in Hα (Figure

6b). An enhanced brightness around both feet is observed as long as the field continues to emerge (Zirin 1972), which is an indication of magnetic energy dissipation.

Large active regions are formed by contributions from several EFRs emerging at different orientations and different times. After 3 to 4 days the AFS are replaced by a system of arches called Field Transition Arches (FTA; Zirin, 1972), which are similar to arch filaments, but are thinner and not very dark. These are formed in places where the magnetic field appears to be almost horizontal. At this time the various EFRs are aligned and have merged forming a single, bipolar active region.

The dynamic characteristics and physical parameters of arch filaments have been studied by several authors (Bruzek 1967, 1969, Frazier 1972, Chou and Zirin 1988, Alissandrakis et al 1990, Georgakilas et al 1990, Tsiropoula et al 1992). Knowledge of the velocity field in AFS is essential in understanding the emergence of the magnetic flux. The "classical" picture of flow is that of ascending motions near the apex and descending motions at the footpoints. Georgakilas et al (1990), assuming a symmetric loop, reconstructed the velocity vector along an arch filament. They found ascending motions at ~ 10 km s^{-1} at the apex of the arches, which are interpreted in terms of their upward expansion and descending motions of ~ 8 km s^{-1} near the footpoints, which is considered as evidence of material draining out of the tube. Tsiropoula et al (1992) also reconstructed the velocity vector and, using Beckers' cloud model, found horizontal velocities of up to 40 km s^{-1} near the footpoints, ascending velocities of ~ 10 km s^{-1} near the apex and descending motions up to 20 km s^{-1} at the footpoints. Chou & Wang (1987) reported another interesting quantity, the separation velocity of the footpoints, which is probably less than 1 km s^{-1}, and is an indication of the separation velocity of emerging opposite poles. Mein et al (1996) obtain an upward velocity of ~ 4 km s^{-1} using a free model to fit their Hα observations of arch filaments.

Although EFRs are of fundamental importance in understanding solar activity their structure and dynamics have not yet been fully understood. One of the major problems is to clarify how magnetic flux is carried from the convection zone to the photosphere and how it expands upwards. Zwaan (1992) suggested that the birth and growth of active regions can be attributed to the emergence of an Ω-shaped loop from a deep-seated toroidal flux strand. After its release from the bottom of the convection zone, its top rises up into the atmosphere within 3 to 4 weeks, if it rises at the Alfvén speed at the local equipartition field strength $B_e q(z)$ (~ 600 G for $v \simeq 3$ km s^{-1}). The downflows observed in the chromosphere and lower in the photosphere have been interpreted by a process called "convective collapse". According to this picture, instabilities at the top of the convection zone enhance the initial downdrafts. As a result the loops evacuate first from the top and subsequently the evacuation is carried deeper down. The high concentration of magnetic fields and the confinement of the individual flux tubes is also not easy to explain. Moreno-Insertis (1992) showed that a flux tube rising from the bottom of the convection zone is expected to expand enormously. van Ballegooijen (1984) proposed a mechanism for the confinement of the static flux loops. According to this, "convective turbulence" leads to a departure from hydrostatic equilibrium, which causes a slight overpressure in

the surrounding convection zone and restricts the expansion of the adiabatically rising tops of the flux loops.

5. Discussion

This review has aimed to display the current knowledge about the properties of different individual structures consisting photospheric and chromospheric active regions, focusing mainly on observational features. Furthermore, special attention is given to the methods of velocity determination and the velocity fields. However, the list of the structures and their properties described is not and could not be exhaustive due to space limitations (e.g. magnetic knots, plages, superpenumbral fibrils, ephemeral active regions etc. are not described). But we think that it is clearly revealed that the coupling of magnetic field and convective motions is fundamental in all phenomena of the atmosphere above the photosphere. This field, emerging from the interior of the Sun into the photosphere and above, creates active regions, the study of which provides important clues for the emergence, evolution and removal of magnetic flux from the deeper layers. Velocity fields are controlled by different physical processes which are usually coupled with the magnetic field, e.g. convection and rotation, magnetic instabilities, magnetic reconnection etc.

It is a common point of view that understanding of individual structures and, especially, their dynamics and their relationship with structures in the overlying and underlying layers is an essential prelude to the understanding and modelling of the global solar atmosphere. In recent years high resolution observations have provided high quality images revealing the fine structure of the various solar features. With the impressive improvements in our understanding of the physical processes involved, in the sophisticated computational techniques used for the analysis of data, in theory (like in non-LTE radiative transfer, in MHD etc) a substantial progress has been achieved. However, a number of contradictions has been revealed even for long-known phenomena. This means that we will not stop to ask for higher and higher spatial and spectral resolution, for technical improvements in the instruments and for improvements in theory, interpretation and modelling.

Acknowledgments. The author gratefully acknowledges Dr C.E. Alissandrakis for the careful reading of the manuscript and his fruitful comments and Dr J.M. Beckers for his suggestions. Figures 2, 5, 6 have been reproduced with the kind permission of Kluwer Academic Publishers.

References

Alissandrakis, C. E., Tsiropoula G. & Mein P. 1990, A&A, 230, 200

van Ballegooijen, A. A. 1984, in Small-Scale Dynamical Processes in Quiet Stellar Atmospheres, NSO-Sacramento Peak, 260

Beckers, J. M., 1964, Ph.D Thesis, Utrecht

Beckers, J. M. & Milkey, R. W. 1975, Solar Phys., 43, 289

Beckers, J. M. 1981, in The Sun as a Star, Jordan S., Monograph series on nonthermal phenomena in stellar atmospheres, NASA SP-450, 11

Berger, T. E., Schrijver, C. J., Shine, R. A., Tardbell, T. D., Title, A. M. & Scharmer, G. 1995, ApJ, 454, 531

Bray, R. J. 1973, Solar Phys., 30, 335

Bruning, D. H. & LaBonte, B. J. 1983, ApJ, 271, 853

Bruzek, A. 1967, Solar Phys., 2, 451

Bruzek, A. 1968, in Structure and development of Solar Active Regions, IAU Symp. 35, Kiepenheuer K.O, Dordrecht:Reidel, 293

Bruzek, A. 1969, Solar Phys., 8, 29

Bruzek, A. 1972, Solar Phys., 26, 94

Canfield, R. C. 1976, Solar Phys., 50, 239

Chapman, G. A., Herzog, A. D. & Lawrence, J. K. 1986, Nature, 319, 654

Chou, D.-Y. & Wang, H. 1987, Solar Phys., 110, 81

Chou, D.-Y. & Zirin, H. 1988, ApJ, 333, 420

Dara, H. C., Alissandrakis, C. E., Zachariadis, Th. G. & Georgakilas A. A. 1997, A&A, 322, 653

Deinzer, W., Hensler, G., Schüssler, M. & Weisshaar, E. 1984, A&A, 139, 435

Denker, C., de Boer C. R., Volkmer, R. & Kneer, F. 1995, A&A, 296, 567

Dunn, R. B. & Zirker, J. B. 1973, Solar Phys., 33, 281

Engvold, O. & Maltby, P. 1968, in Mass Motions in Solar Flares and Related Phenomena, Y. Ohman, Nobel Symp. 9, 109

Foukal, P., Fowler, L. & Livshits, M. 1983, ApJ, 267, 863

Foukal, P., & Fowler, L. 1984, ApJ, 281, 442

Frazier, E. N. 1972, Solar Phys., 26, 130

Frazier, E. N. & Stenflo, J. O. 1978, A&A, 70, 789

Georgakilas, A. A., Alissandrakis, C. E. & Zachariadis, Th. G. 1990, Solar Phys., 129, 277

Gouttebroze, P., Heinzel, P. & Vial, J.-C. 1993, A&A, 99, 513

Gu, X.M., Ding, Y.J., Luo, Z. & Schmieder, B. 1997, A&A, 324, 289

Harvey, K. L. & Martin, S. 1973, Solar Phys., 32, 389

Heinzel, P. & Schmieder, B. 1994, A&A, 282, 939

Heinzel, P. 1995, A&A, 299, 563

Howard, R. W. & Stenflo, J. O. 1972, Solar Phys., 22, 402

Keil, S. L. & Muller, R. 1983, Solar Phys., 87, 243 A&A, 233, 583

Kiepenheuer, K.O, 1968, in Structure and development of Solar Active Regions, IAU Symp. 35, Kiepenheuer K.O, Dordrecht:Reidel, 3

Kitai, R. 1983, Solar Phys., 87, 135

Kitai, R. & Muller, R. 1984, Solar Phys., 90, 303

Koutchmy, S. & Stellmacher, G. 1978, A&A, 67, 93

Koval, A. N. & Severny, A. B. 1970, Solar Phys., 11, 276

Kulander, J. L. & Jefferies, J. T. 1966, ApJ, 146, 194

Kurokawa, H., Kawaguchi, I., Funakoshi, Y. & Nakai, Y. 1982, Solar Phys., 79, 77

Leighton, R. B., Noyes, R. W. & Simon G. W. 1962, ApJ, 135, 474

von der Lühe, O. 1994, A&A, 281, 889

Mehltretter, J. P. 1974, Solar Phys., 38, 43

Mein, N. & Schmieder, B. 1981, A&A, 97, 310

Mein, N., Mein, P., Heinzel, P., Vial, J.-C., Malherbe, J. M. & Staiger, J. 1996, A&A, 309, 275

Mein, P. 1971, Solar Phys., 20, 3

Mein, P. 1977, Solar Phys., 54, 45

Mein, P., Mein, N., Malherbe, J. M. & Dame, L. 1987, A&A, 177, 283

Mein, P. & Mein, N. 1988, A&A, 203, 162

Mein, P. 1991, A&A, 248, 669

Mein, P., 1992, in Solar Observations: Techniques and interpretation, Sánchez F., Collados M. & Vázquez M., Cambridge University Press, 181

Mein, P., Démoulin, P., Mein, N., Engvold, O., Molowny-Horas, R., Heinzel, P. & Gontikakis C. 1996, A&A, 305, 343

Moreno-Insertis, F. 1992, Sunspots:Theory and Observations, J. H. Thomas & N. O. Weiss, Dordrecht:Kluwer, NATO ASI Series, vol 375, 385

Muller, R. 1977, Solar Phys., 52, 249

Muller, R. 1983, Solar Phys., 85, 113

Muller, R. & Mena, B. 1987, Solar Phys., 112, 295

Muller, R., Roudier, Th. & Hulot, J. C. 1989, Solar Phys., 119, 229

Muller, R., Roudier, Th., Vigneau, J. & Auffret, H. 1994, A&A, 283, 232

November, L. J., Simon, G. W., Tardbell, T. D., Title, A. M. & Ferguson, S. H. 1987, in Theoretical Problems in High Resolution Solar Physics II. NASA CP-2483, Athay R. G. & Spicer D., Washington, DC:NASA, 121

November, L. J. & Simon, G.W. 1988, ApJ, 333, 427

Oster, L., Schatten, K. & Sofia, S. 1982, ApJ, 256, 768

Paletou, F. & Auer, L.H. 1995, A&A, 297, 771

Paletou, F. 1996, A&A, 311, 708

Parker, E. 1990, Mechanisms of Chromospheric and Coronal Heating, P. Ulmschneider, E. R. Priest & R. Rosner, Berlin:Springer, 615

Payne, T. 1993, Bull. American Astron. Soc., 183

Roy, J.-R. 1973, Solar Phys., 32, 139

Roy, J.-R. & Leparskas, H. 1973, Solar Phys., 30, 449

Rust, D. M. 1968, in Structure and development of Solar Active Regions, IAU Symp. 35, Kiepenheuer K.O, Dordrecht:Reidel, 77

Rust, D. M. & Keil, L. 1992, Solar Phys., 140, 55

Schmieder, B. & Mein, N. 1980, A&A, 84, 99

Schüssler, M. 1987, in The role of Fine-Scale Magnetic Fields on the Structure of the Solar Atmosphere, Shröter, E. H., Vázquez, M. & Wyller, A. A., Cambridge University Press

Schüssler, M. 1992, in The Sun: A Laboratory of Astrophysics, J. T. Schmelz & J. C. Brown, Dordrecht:Reidel, NATO ASI Series, Vol. 373, 191

Severny, A. B. 1965, in The Solar Spectrum, C. de Jager, Dordrecht: Reidel, 221

Severny, A. B. 1968, in Mass Motions in Solar Flares and Related Phenomena, Y. Ohman, Nobel Symp. 9, 109

Sofia, S., Oster, L. & Schatten, K. 1982, Solar Phys., 80, 87

Solanki, S. K. 1986, A&A, 168, 311

Solanki, S. K. 1993, Space Sci.Rev., 63, 1

Spruit, H. C. 1976, Solar Phys., 50, 269

Spruit, H. C., Nordlund, Å, & Title, A. M. 1990, ARA&A, 28, 263

Steinegger, M., Brandt, P. N. & Haupt, H. F. 1996a, A&A, 310, 635

Steinegger, M., Vázquez, M., Bonet, J. A. & Brandt, P. N. 1996b, ApJ, 461, 478

Steiner, O. & Stenflo, J. O. 1990, in Solar Photosphere: Structure, Convection and Magnetic Fields, J. O. Stenflo, IAU Symp. 138, Dordrecht:Kluwer

Stenflo, J. O. 1973, Solar Phys., 32, 41

Stenflo, J. O., Harvey, J. W., Brault, J. W. & Solanki, S. K. 1984, A&A, 131, 333

Stenflo, J. O. & Harvey, J. W. 1985, Solar Phys., 95, 99

Strous, L. H., Scharmer, G., Tarbell, T. D., Title, A. M. & Zwaan C. 1996, A&A, 306, 947

Title, A. M., Topka, K. P., Tarbell, T. D., Schmidt, W., Balke, C. & Scharmer, G. 1992, ApJ, 393, 782

Topka, K. P., Tarbell, T. D. & Title, A. M. 1992, ApJ, 396, 351

del Toro Iniesta, J. C., Collados, Sánchez Almeida, M., Martinez Pillet, V. & Ruiz Cobo, B. 1990, A&A, 233, 570

Tsiropoula, G., Georgakilas, A. A., Alissandrakis, C. E. & Mein, P. 1992, A&A, 262, 587

Tsiropoula, G., Alissandrakis, C. & Schmieder, B. 1993, A&A, 271, 574

Tsiropoula, G., Alissandrakis, C. & Schmieder, B. 1994, A&A, 290, 285

Tsiropoula, G. & Schmieder, B. 1997, A&A, 324, 1183

Wang, Y.-M., Nash, A. G. & Sheeley, N. R., Jr. 1989, Science, 245, 712

Wöhl, H., 1992, in Solar Observations: Techniques and interpretation, Sánchez, F., Collados, M. and Vázquez, M., Cambridge University Press, 147

Yi, Z. & Engvold, O. 1993, Solar Phys., 144, 1

Yi, Z. & Molowny-Horas, R. 1995, A&A, 295, 199

Zachariadis, Th., Alissandrakis, C. E. & Banos, G. 1987, Solar Phys., 108, 227

Zirin, H. 1972, Solar Phys., 22, 34

Zwaan, C. 1992, in Sunspots:Theory and Observations, J. H. Thomas & N. O. Weiss, Dordrecht:Kluwer, NATO ASI Series, vol 375, 75